

Article

Active Tectonics along the South East Offshore Margin of Mt. Etna: New Insights from High-Resolution Seismic Profiles

Giovanni Barreca ^{1,*} , Marta Corradino ² , Carmelo Monaco ¹  and Fabrizio Pepe ² 

¹ Dipartimento di Scienze Biologiche, Geologiche e Ambientali, University of Catania, Corso Italia, 57, 95129 Catania, Italy; cmonaco@unict.it

² Dipartimento di Scienze della Terra e del Mare (DISTEM), University of Palermo, Via Archirafi, 20/22, 90123 Palermo, Italy; marta.corradino@unipa.it (M.C.); fabrizio.pepe@unipa.it (F.P.)

* Correspondence: g.barreca@unict.it; Tel.: +39-095-719-5703

Received: 6 December 2017; Accepted: 6 February 2018; Published: 8 February 2018

Abstract: The offshore margin of Mt. Etna has been shaped by Middle Pleistocene to Holocene shortening and extension and, more recently, by gravity-related sliding of the volcanic edifice. These processes have acted contemporaneously although the gravitational component largely prevails over the tectonic one. In order to investigate this issue, we focused on the main role of active tectonics along the south-eastern offshore of Mt. Etna by means of marine high-resolution seismic data. Seismic profiles revealed post-220 ka sedimentary deposits unconformably overlaying the Lower-Middle Pleistocene Etnean clayey substratum and volcanics of the Basal Tholeiitic phase and the Timpe phase. Offshore Aci Trezza-Catania, the architecture of the sedimentary deposits reflects syn-tectonic deposition occurred into “piggy-back” basin setting. Shortening rate was estimated at ~0.5 mm/a since ~220 ka. Asymmetric folding also involves post Last Glacial Maximum deposits, evidencing that compressional deformation is still active. In the continental slope, a belt of normal faults offset the Lower-Middle Pleistocene Etnean clayey substratum and younger deposits, also producing seafloor ruptures. Thrust and fold structures can be related to the recent migration of the Sicilian chain front, while extensional faults are interpreted as part of a major tectonic boundary located in the Ionian offshore of Sicily.

Keywords: Mt. Etna; seismic investigation; active tectonics; Sicilian thrust-belt; Ionian Sea

1. Introduction

Mt. Etna, located in southern Italy (Figure 1), is one of the most studied volcanoes in the world due to its frequent activity in a densely populated area. The volcanic edifice has grown within an intricate geodynamic framework and its origin has been related to the activity of regional-scale tectonic boundary in eastern Sicily [1]. Accordingly, crustal faulting and associated fracturing favoured magma ascent through the lithosphere along the Ionian coast of Sicily in the last 500 ka. Volcanics have accumulated to form the composite Mt. Etna volcano reaching ~3.350 m above sea level [2].

Currently, the volcanic edifice is affected by deformation related to (a) volcano dynamics (inflation-deflation); (b) volcano-tectonic processes (dike-induced ground fracturing in the summit area); (c) regional normal-oblique faulting; and (d) flank gravitational instability (see [3] for an overview). In particular, gravity-related deformation has given rise to a large sliding area with associated ground ruptures affecting the entire eastern slope of the volcano [4,5]. As evidenced by geodetic data [6,7] and interferometric studies [8–10], the sliding area is characterized by a fairly seaward motion of several blocks. The gravitational deformation is accommodated by shallow discontinuities at its northern and southern boundaries and pre-existing tectonic structures [3].

Several seafloor scarps, recently evidenced by multibeam data acquired along the Ionian continental shelf [11,12], have been related to internal deformation of the mobile blocks. However, large-scale active tectonic lineaments [13,14] pose questions on their role in the deformation of the south-eastern flank and offshore margin of Mt. Etna.

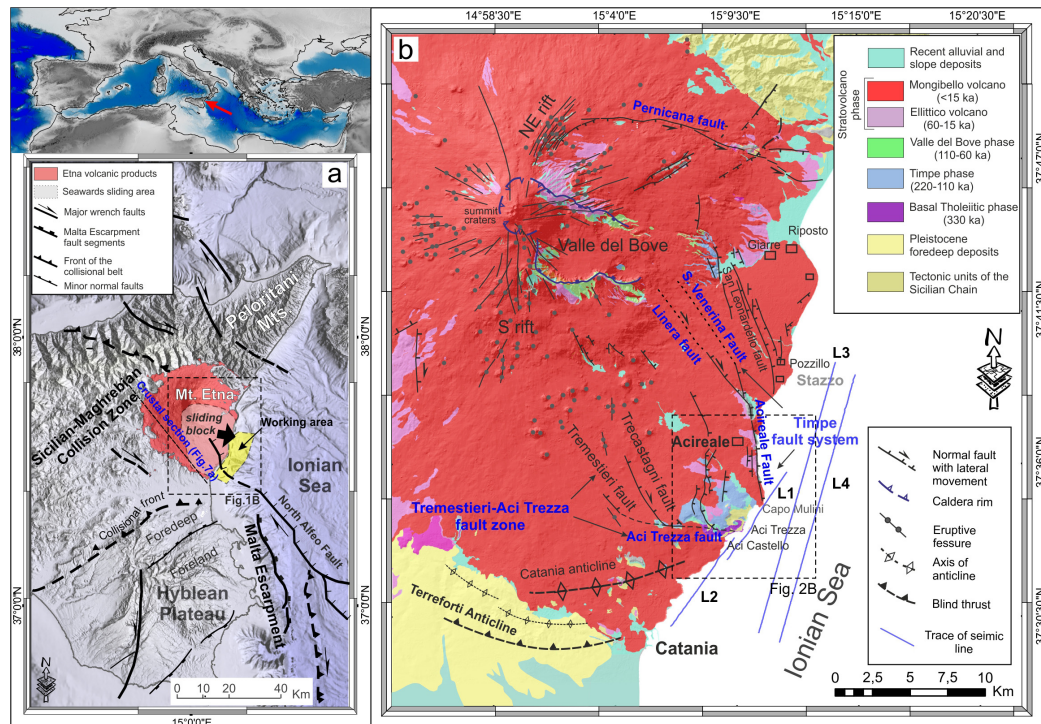


Figure 1. (a) Tectonic sketch-map of eastern Sicily and Ionian offshore. The Mt. Etna Volcano (red area) lies mainly at the top the Sicilian-Maghrebian Collision Zone, a fold and thrust belt sandwiched between the Peloritani Block in the North and the Hyblean Foreland in the south. Major tectonic boundaries in the Ionian Sea (e.g., the Malta Escarpment and the North Alfeo Fault [13] appear to merge in the Mt. Etna area); (b) Structural framework of the eastern and southern flanks of Mt. Etna, showing a complex deformation field resulting from volcano-tectonic processes, sliding block dynamics and regional tectonics. L1–L4, high-resolution seismic dataset used in this study.

Based on geodetic measurements along several structures [3], the rate of the gravitational deformation is one order greater than the tectonic component, which, for this reason, could be masked. Deformation affecting the eastern and southern flank of the volcano and its offshore sector has been explained by sliding dynamics [8–10]. Nevertheless, uplifted paleo-shorelines at the footwall of normal faults, documented at the SE sector of the volcano [15], suggest that the tectonic signal is prevailing over the non-tectonic one. Moreover, active thrusting and folding at the southern border of the volcanic edifice [16] are coherent with the ~N–S regional compression, still affecting the frontal sector of the Sicilian-chain [17].

In this paper, we investigate the active tectonics deformation in the south-eastern offshore sector of the Mt. Etna volcanic edifice, between Catania harbour and the Stazzo village to the north (Figure 1b), by using high-resolution seismic reflection profiles and published seafloor bathymetry [11]. Our profiles cross the seaward prolongation of some well-known fault [3,4,18–21] and fold [10,16,17,22] systems mapped on-land, in order to better constrain mechanism and timing of active tectonic deformation processes. Moreover, the new faults documented on seismic profiles have been framed in the regional geodynamic offshore eastern Sicily.

2. Regional Setting

2.1. Geodynamic Framework

Mount Etna volcano lies at the front of the Sicilian-Maghrebian thrust belt and on the Early-Middle Pleistocene foredeep clayey succession (Figure 1a) deposited on the flexured margin of the Hyblean foreland [19]. This succession is currently deformed by detachment folds related to the recent frontal migration of the thrust belt, as response to the approximately N–S compressive regional tectonic regime [16,17,22–24]. Since the Middle Pleistocene, contractional structures have been coupled with oblique extensional faults formed across the western Ionian Basin. These faults form a lithospheric boundary characterized by strong seismicity and active volcanism, which extends from Aeolian Islands to eastern Sicily offshore, including the Malta Escarpment [1,13,14,25–28].

The Malta Escarpment Fault System has been considered to have a primary role in the origin of Mt. Etna due to its location, just south-east of the volcano and its recent transtensional kinematics [18,29–31]. However, swath-bathymetry and multichannel seismic data recorded offshore Mt. Etna [13,14,32–34] revealed the existence of other active fault systems in the western Ionian Sea. One of these (the NW-SE trending and transtensional North Alfeo Fault System [13]; see Figure 1a for location) joins obliquely the Malta Escarpment Fault System. According to [14], this belt is primarily associated with the relative motion of Africa and Eurasia since it accommodates diverging motions in adjacent western Ionian compartments.

2.2. Onland Sedimentary and Volcanic Stratigraphy

The sedimentary substratum of the volcanic edifice outcrops south of Mt. Etna and locally along the Ionian shoreline, at the front of the Sicilian fold and thrust belt (Figure 1b). It is made up of a Lower-Middle Pleistocene foredeep succession of marine bluish marly silty clays with rare intercalations of fine-grained sands and volcanics (see below), up to 600 m thick, evolving upwards to tens of meters of cross-bedded yellowish quartzose sands (locally named Terreforti) of fluvial-deltaic environment [35]. The latter, referred to as the Mindel-Riss interglacial stage by Reference [36], are unconformably overlain by terraced sands and/or conglomerates of coastal-alluvial origin, whose absolute age is between 240 and 60 ka [37].

The volcanics consist of an earlier Basal Tholeiitic phase [2,38] characterized by discontinuous and scattered fissural volcanic activity, occurred in the foredeep basin between 500 ka and 330 ka, including the intrusion of the Aci Trezza laccolith (remnants outcrop in the small rocky islets). The volcanism in the Mt. Etna region was concentrated along the Ionian coast between 220 and 120 ka (the Timpe phase [2,38]), represented by plugs of columnar lavas and proximal pyroclastic deposits, outcropping at the bottom of the Acireale Fault Scarp (Figure 1b), along N–S trending eruptive fissures [39]. In this time span, the extensional tectonics of the Ionian margin of Sicily [18,19,40] favoured the ascent of alkaline magma in the Mt. Etna region, transforming the previous scattered fissural volcanism into an almost continuous volcanic activity that shifted westward to build the bulk of the present edifice since 100 ka. The Valle del Bove (100–60 ka), the Ellittico (60–15 ka) and the Mongibello (15–0 ka) volcanic centres have developed during this time span (Figure 1c, [2,19,38]).

2.3. Active Tectonics in South-Eastern Sector of Mt. Etna

The lower eastern flank of Mt. Etna is characterized by several morphological scarps formed by Middle Pleistocene to Holocene normal-oblique faulting (the Timpe Fault System, Figure 1b [19,40]). The NNW-SSE trending Acireale Master Fault morphologically controls a 10 km-long coastal stretch, forming an up to 200 m high cliff, with a vertical slip-rate of ~4.3 mm/yr in the last 35 ka [40]. Northwards, some segments of the Timpe Fault System are aligned in a NW-SE direction with striated fault planes indicating right-lateral transtensional motion (e.g., Santa Venerina and Linera faults [19,20]). Shallow-depth seismicity (5–6 km), capable of producing earthquakes with magnitude up to 4.5 and oblique (right lateral-normal) focal mechanisms, is associated with this system [41–43].

The Timpe fault system has been considered one of the northernmost segments of the NNW-SSE oriented Malta Escarpment Fault System [18] responsible of the footwall uplift of the coastal sector of south-eastern Sicily, during the Middle-Late Pleistocene [26]. The uplift of the region, with a maximum rate of ~ 1.4 mm/yr that progressively decreasing southwards, is evidenced by a flight of marine terraces [26]. Conversely, the Pleistocene foredeep clayey deposits and the overlying coastal-alluvial deposits, located along the southern margin of the volcano, have been involved in the Late Pleistocene compressive deformation (see below [16,22,24,37]). GPS measurements over the last 20 years have revealed a shortening rate of ~ 5 mm/yr along a NNW-SSE oriented axis of compression, consistent with focal mechanism of deep earthquakes generated by the collisional front of the chain [17].

The uplift of the volcanic edifice, related to volcano-tectonic regional processes and/or local deformation along faults [44–49], is locally interrupted by subsidence related to the flank sliding, measured at docks and other manmade structures (up to 15 mm/yr [15]) and by acceleration at the footwall of the Acireale fault or along the hinge of growing anticlines in the Aci Trezza coastal sector (up to 3 mm/yr [15]). Interferometric data have highlighted the current growth of a large \sim W-E oriented anticline, the Catania Anticline, extending from the north-western outskirts of Catania to Aci Trezza (Figure 1b [9]). Evidence of active folding related to the Catania Anticline is difficult to observe, because of its location in a volcanic and intensely populated area. However, differential ground motion based on interferometric data [9,10] matches with morphostructural field data, which suggest active vertical deformation [17]. The Catania Anticline is characterized by a maximum uplift rate of ~ 10 mm/yr along the hinge zone. The aseismic uplift of the Catania Anticline has been interpreted either as the result of gravitational spreading [9,10] of the volcanic edifice or as the detachment folding related to a shallow thrust migrating within the foredeep deposits at the chain front [17]. The latter interpretation is preferred considering that this structure is near-parallel to the Terreforti Anticline (Figure 1b), a ~ 10 km long thrust propagation fold developed at the front of the chain between 240 and 200 ka [37].

Multiple studies [3,21,50] indicate that the eastern flank of Mt. Etna Volcano has been sliding seaward (Figure 1a). The sliding area is confined to the west by the NE and S rift zones passing through the summit craters, to the north by the left-lateral Pernicana Fault and to the south by the right-lateral Tremestieri-Aci Trezza Fault Zone (Figure 1b). The gravitational deformation interacts with the fault systems located in the lower slopes [3,21] and offshore [11,12,51]. According to the shallow sliding model [3,4,21], the eastern mobile sector is dismembered into minor sub-blocks of volcanics slowly sliding eastwards under their own weight, accommodated by seaward dipping detachment surfaces within the sedimentary substratum. At Mt. Etna, slope movements have been considered active since ~ 14 ka [52] at velocities of several cm/yr. However, such movements do not match morphological, tectonic and geological data, especially along the Aci Trezza coastline where only local incipient fracturing occurs [3,15]. Nevertheless, some authors [12] assign great importance to the southern boundary of the sliding block, inferring its continuation in the Aci Trezza offshore.

3. Materials and Methods

Over 400 km of high-resolution, reflection seismic data were recorded offshore Mt. Etna, along the continental shelf and upper slope, in August 2014. We present a subset of these data, consisting of two NE-SW and two NNE-SSW oriented seismic profiles between the Catania harbour and the Stazzo village to the north (Figure 1b). The acoustic source for seismic prospecting was a 1 kJ Geo-Source Sparker, with a multi-tip Sparker array and a single-channel streamer having an active section of 2.8 m. Navigation was controlled by a DGPS system.

Processing of seismic data included: (a) true amplitude recovery using a T^2 spherical divergence correction; (b) band-pass (300–2000 Hz) “finite impulse response” filter using a filter length of 256 samples; (c) de-ghosting; (d) swell-filter; (e) deconvolution; (f) trace mixing of three traces for enhancing horizontal signal; (g) time variant gain to boost amplitudes of deeper arrivals; (h) mutes

to eliminate the signal noise on the water column. Signal penetration was found to exceed 250 ms two-way time (t.w.t.).

The reconstruction of the depositional architecture of seismic-stratigraphic units was based on seismo- and sequence-stratigraphic analysis, coupled with spatial correlations between volcanic deposits inferred from seismic data and those outcropping on-land. Following the analysis of acoustic facies, the sediment thickness, depth of unconformities and apparent dip of stratigraphic surfaces were derived from t.w.t. (ms) to depth (m) conversion of seismic horizon using velocities of 1515 m/s, 1650 m/s and 1800 m/s for the water column, post- and pre-Last Glacial Maximum (LGM) deposits, respectively. These values were derived from sound velocity profiles and sonic log data acquired in coeval deposits along similar offshore settings [53,54].

4. Results and Interpretations

4.1. Seismic Stratigraphy

We identified four seismic stratigraphic units on the NE-SW oriented line L1 (Figure 2a,b) on the basis of their bounding discontinuities, strata architecture and seismic characters (e.g., amplitude, lateral continuity and frequency of internal reflectors [55]). The seismic stratigraphic units were labelled from older to younger as Unit A, B, C and D. Ages were assigned to the seismic units based on well documented, age-constrained volcanics [2] and sedimentary deposits outcropping on-land [35] along the coastline (Figure 2c).

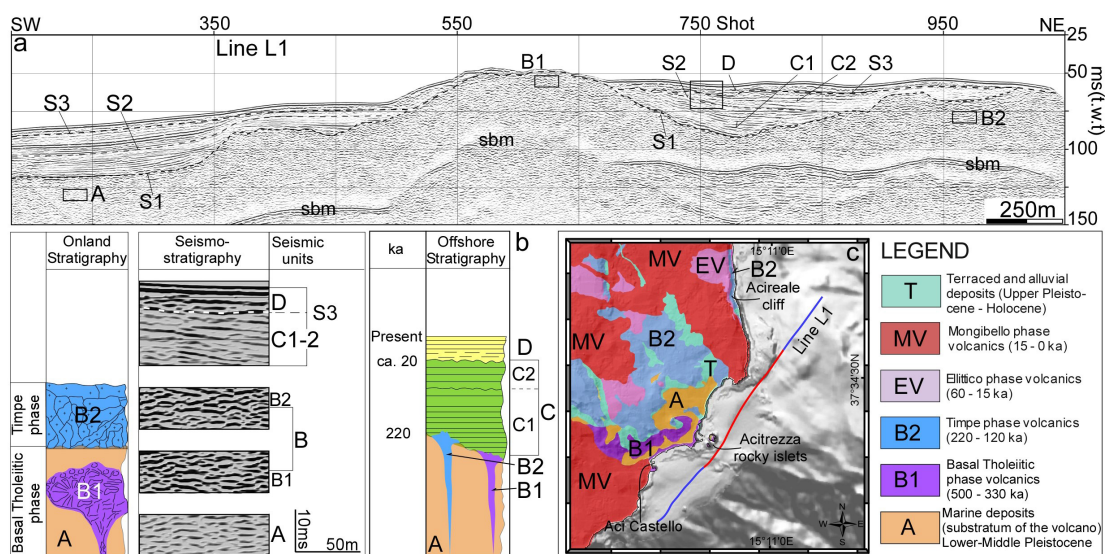


Figure 2. (a) Geometry and distribution of detected seismic units along a portion of line L1 (red haloed portion in Figure 2c); (b) A seismo-stratigraphic model reconstructed from seismic facies analysis; and (c) correlation of the seismic units with age-constrained volcanics and sedimentary deposits outcropping on-land (age of volcanics from [2]). S1, S2 and S3 are erosional surfaces (see text for explanation); sbm: sea bottom multiple.

Unit A is characterized by a succession of high-frequency, low- to medium-amplitude, discontinuous reflections (Figure 2a,b). The top of unit A, when detectable, is an erosional surface (S1 in Figure 2a).

Unit B is characterized by discontinuous reflections of high-amplitude (Figure 2b). The upper boundary of this unit is a high-amplitude, discontinuous seismic reflector characterized by a rough morphology and numerous diffractions. Locally, Unit B is truncated by the S1 erosional surface. Unit B can be subdivided into two sub-units B1 and B2, which are interpreted as the seismic expression of volcanics erupted during the Basal Tholeiitic phase and the Timpe phase, respectively.

Unit C is characterized by a succession of stratified, high-frequency, low- to medium-amplitude, discontinuous or locally continuous reflections (Figure 2b). The bottom and top of unit C are defined by the S1 and S3 erosional surfaces, respectively. Unit C is locally subdivided into two sub-units, C1 and C2, characterized by a parallel and divergent internal configuration of reflectors, respectively. The reflector S2 separates these sub-units (Figure 2a).

Unit D is represented by high-frequency, well-defined, moderate-amplitude reflections with partial lateral continuity and parallel geometry (Figure 2b). The bottom and top of Unit D are defined by the S3 erosional surface and the seafloor, respectively.

A distinctive seismic feature was also identified, corresponding to fluid intrusions and labelled as FI (Figure 3e).

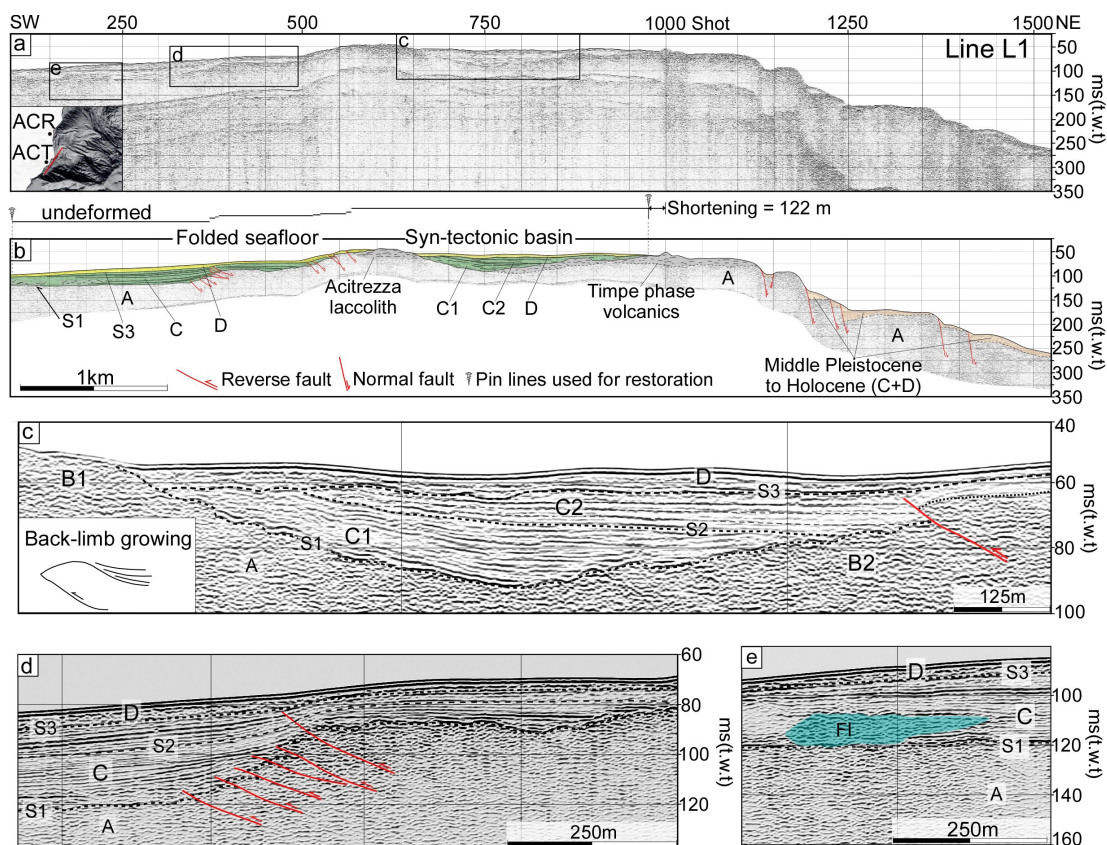


Figure 3. (a) The offshore margin of Mt. Etna as imaged along line L1 (see Figure 1b for location); (b) Tectonic interpretation of line L1 showing contractional (SW) and extensional (NE) structural features (A, B, C, D: see Figure 2 for abbreviations). C1 and C2, syn-tectonic deposits; S1, S2 and S3, erosional surfaces. Cross-section restoration of the contractional structures on line L1 shows estimated shortening of 122 m; (c) Syn-tectonic basin NE of the Acitrezza laccolith. Inset shows geometry of growth folding; (d) Closely spaced, southeast vergent reverse faults with small displacements (red lines) affecting the Acitrezza laccolith and Unit C. Both reverse and normal faults offset post-220 ka deposits and/or have folded the seafloor, reflecting ongoing activity; (e) FI, mud/fluid intrusion; ACR: Acireale; ACT: Aci Castello.

4.2. Depositional Architecture of Seismic-Stratigraphic Units

The lowest sedimentary package recognized on seismic lines (Unit A, Figures 2–6) correlates to the Lower-Middle Pleistocene Etnean clayey substratum, largely outcropping along the coastline between Aci Trezza and Aci Castello (Figure 1b). Overall, the Lower-Middle Pleistocene deposits are truncated by a well-developed erosional surface (S1 in Figures 3–6), formed during sea-level lowstand stages as a consequence of subaerial exposure of the continental platform.

The top of the Lower-Middle Pleistocene Etnean clayey substratum (S1) appears horizontal or slightly ($<0.5^\circ$) seaward dipping along the continental shelf (Figures 3 and 4). Close to Aci Trezza, the measured difference in depth of the S1 erosional surface in the flanks of the Catania Canyon is ~ 28 m (Figure 4b). Based on the consideration that the S1 originally formed as a flat and continuous out-of-water surface, this offset has been probably caused by Middle Pleistocene to Holocene faulting (e.g., south-verging thrusting). On the continental slope, extensional fault-controlled basins occur and S1 is tilted and/or displaced according to the faults movements. Towards the NNE it appears as an uneven surface as consequence of landslide processes (Figures 5 and 6).

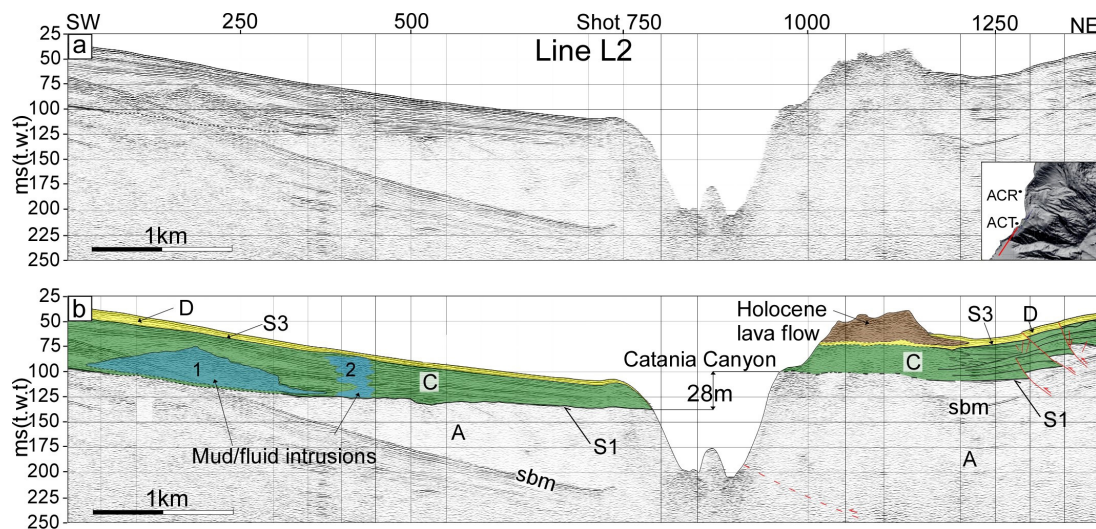


Figure 4. (a) Un-interpreted; and (b) interpreted line L2 showing reverse faulting, extending from the seafloor into the basement Unit A (see Figure 1b for location). Along the SW sector, Pleistocene-Holocene sediments are tilted toward the Catania Canyon, with a displacement of ~ 28 m. Mud/fluid intrusions (1 and 2), deforming the units C and D, are evident. Red dashed line: inferred thrust fault. ACR: Acireale; ACT: Aci Trezza; S1 and S3, erosional surfaces; sbm, sea bottom multiple (A, B, C, D: see Figure 2 for other abbreviations).

The seismic signature of sub-units B1 and B2 is typical of volcanic rocks (Figure 2c). Volcanics of sub-unit B1 are exposed at the seafloor in the central portion of line L1 (Figure 3b), just east of the Aci Trezza rocky islets and interpreted as the seaward prolongation of the volcanics of the Basal Tholeiitic phase outcropping in the Aci Trezza rocky islets (~ 330 ka [2]). Volcanics of sub-unit B2 are recognized in the NE part of line L1 (around shot 1000, Figure 3b), close to the area where the Timpa di Don Masi formation (~ 220 ka [2]) is widespread. Consequently, we associate volcanics of sub-unit B2 with this formation.

The Unit C lies unconformably on top of the Lower-Middle Pleistocene Etnean clayey substratum as well as overlays the volcanics of both sub-units B1 (~ 330 ka [2]) and B2 (~ 220 ka [2]) (Figure 3c). Therefore, it is proposed a post-220 ka age for unit C. On the continental shelf, Unit C is a well-bedded sedimentary succession that can be internally divided into two sub-units, namely C1 and C2, by the reflector S2 (Figure 3c), which likely corresponds to a syn-tectonic erosional surface. The lower sub-unit consists mostly of parallel reflectors, while the upper sub-unit has reflectors that diverge towards the NE, demonstrating syn-tectonics deposition. Units C and D are separated by a well-developed erosional unconformity (S3 in Figures 3 and 4) interpreted as having formed during the last glacial sea level fall and lowstand, ~ 120 m below the present level [56], between ~ 90 ka [57] and ~ 20 ka [58–60]. The thickness of units C and D is variable, depending on the tectonic regime acting in the different sectors at the time of their deposition. On the continental shelf, the thickness of Unit C varies from ~ 47 m to less than 10 m. Units C and D are indistinguishable on the continental slope. Overall, their thickness varies from ~ 60 m to few meters inside the fault controlled basin (Figures 5 and 6). The most

recent Unit D overlays the S3 erosional surface (Figures 3 and 4). Therefore, it is interpreted as having formed during the transgressive and high-stand stages of the last eustatic cycle. On the continental shelf, unit D shows a quite constant thickness of ~5–6 m.

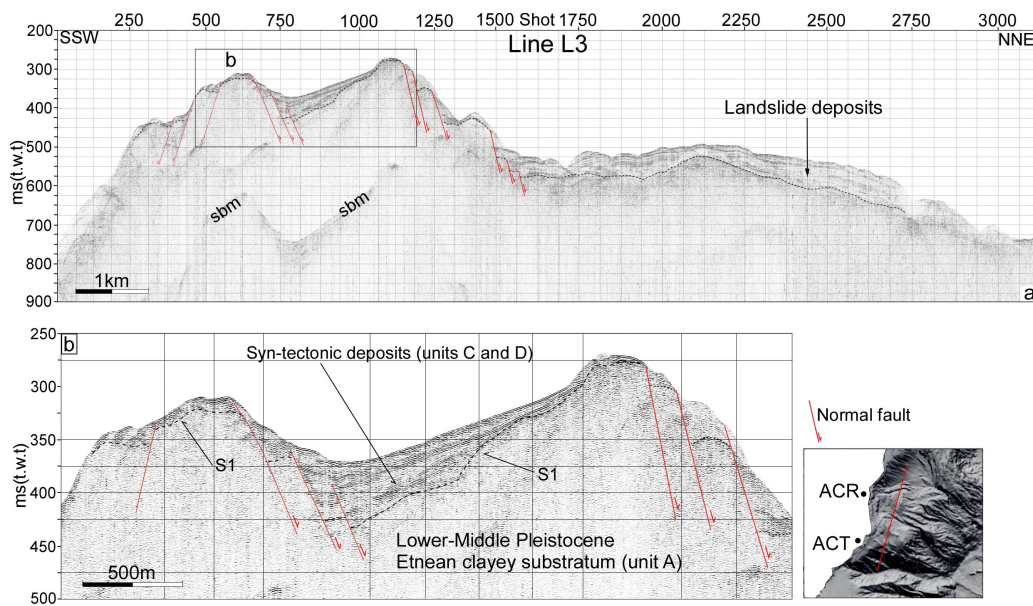


Figure 5. (a) interpreted line L3 showing a set of normal faults controlling the seafloor morphology (see Figure 1b for location); (b) Recent sediments within the wedge-shaped basin suggest syn-sedimentary activity on these faults ACR: Acireale; ACT: Aci Trezza; S1: erosional surface; sbm: sea bottom multiple.

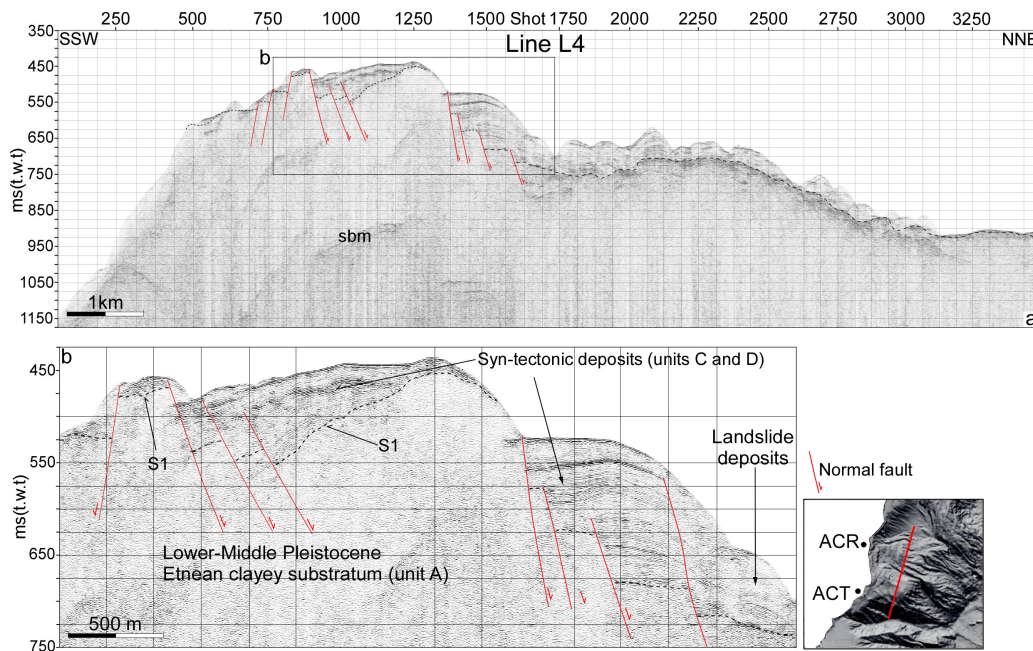


Figure 6 Barreca et al.

Figure 6. (a) Interpreted NNE-SSW trending L4 line showing the offshore prolongation of the NW-SE-trending, mainly NNE-dipping normal faults, also recognized on line L3 (see Figure 1b for location). Faults displaced Middle Pleistocene to Holocene deposits also affecting the seafloor; (b) Box b displays part of the line at smaller scale. ACR: Acireale; ACT: Aci Trezza; S1: erosional surface; sbm: sea bottom multiple.

Mud/fluid intrusions have been detected in the shelf deposits (FI in Figure 3e). Their intrusive nature is suggested by sharply truncated reflectors and forced folding in the hosting seismic units. Southwest of the Catania Canyon these bodies exhibit highly irregular to discontinuous internal reflection patterns (Figure 4b). Moreover, mud/fluid intrusions display striking similarities with complex and stacked single mud volcano edifices, documented in the Western Alborán Sea by [61].

4.3. Deformation Pattern

Several faults are observed along the south-eastern sector of Mt. Etna. Although they rarely show displacements larger than some meters, they document tectonic regime in the region since the Middle Pleistocene. In the continental shelf, geometry of displaced reflectors (including S1 and S2) clearly indicate the occurrence of small reverse faults locally propagating upwards to dislocate Unit C (Figure 3d). Despite the sea floor not being clearly displaced, it appears gently folded. In fact, the entire succession is folded by a southeast-verging anticline in correspondence of the Aci Trezza laccolith (Figure 3b, shots 500–650). Furthermore, S1 appears to be folded close to the shoreline near Acitrezza (Figure 3c, shots 650–750). In the overlying Unit C, internal reflectors diverge towards the NE and on-lap the shield-shaped volcanics of the Timpe phase (unit B2). Diverging reflectors/strata are more evident within the sub-unit C2, whereas they are less marked downwards, within the sub-unit C1 (Figure 3c). Overall, reflectors of Unit C suggest syn-tectonic deposition within small piggy-back basins. It is also worth to note that the volcanics of the Timpe phase have been involved into contractional deformation.

The S1 erosional surface (see Section 4.2) was used as reference horizon (Figure 3b) in order to calculate amount and rate of long-term horizontal component of motion related to the fold propagation. An age of 220 ka was assigned to this horizon, by considering that Unit C unconformably overlies volcanic products that correlate with those erupted on-land during this period (Timpa di Don Masi formation, 220 ka old [2]). 2D restoration of the reference horizon S1 was performed by using the Move software. It was firstly unfolded to the regional dip (assumed flat) adopting the simple shear unfolding algorithm. The pre-deformed length of the reference horizon (Figure 3b) was finally obtained also by back-deforming fault displacements. This method allowed us to obtain a total shortening of ~122 m (Figure 3b), and, accordingly, a shortening rate of ~0.5 mm/yr in the last 220 ka. The resulting value is probably underestimated since the trend of the seismic line is not perpendicular to the orientation of the tectonic structures (see Figure 7c in Section 5).

A structural setting similar to the central-southern part of line L1 is displayed on line L2 where reflectors of unit C are dislocated by south-verging reverse faults in the north-eastern portion of the line (Figure 4, shots 1100–1400). The uppermost part of unit C is mainly preserved in the footwall block, with internal reflectors progressively on-lapping the lowermost deformed part of the unit. A ramp anticline has developed at the hanging-wall where folding has also deformed the seafloor. Post-LGM deposits (unit D) widely occur in the southwestern portion of line L2 where they are gently tilted towards the northeast. Spatial correlation between structures along lines L1 and L2 suggests an ENE-WSW orientation for these fold and thrust structures (see Figure 7).

In the northern-most portion of line L1, a belt of active normal faults affects the Lower-Middle Pleistocene Etnean clayey substratum (Unit A) and younger deposits, also producing significant ruptures on the seafloor (Figure 3b, shots 1100–1500). Fracturing is currently favouring fluid ascent (Figure 3b, shot 1000). Active extensional tectonics have also been detected along lines L3 and L4 (Figures 5 and 6) that show the occurrence of a bathymetric high, just northeast of the Catania Canyon, controlled by a NW-SE trending system of extensional faults. The most prominent structure, which forms a significant scarp on the seafloor, bounds north-eastwards the ridge and consists of a high-angle, NNE-dipping, normal fault displacing Middle Pleistocene to Holocene deposits.

Middle Pleistocene to Holocene deposits widely occur on the down-faulted block where they are preserved within triangular-shaped basins and at the footwall (Figures 5 and 6). Wedge geometry

and growing strata suggest a recent syn-sedimentary activity of this fault system that well correlates on-land with the Timpe Fault System (Figure 1b).

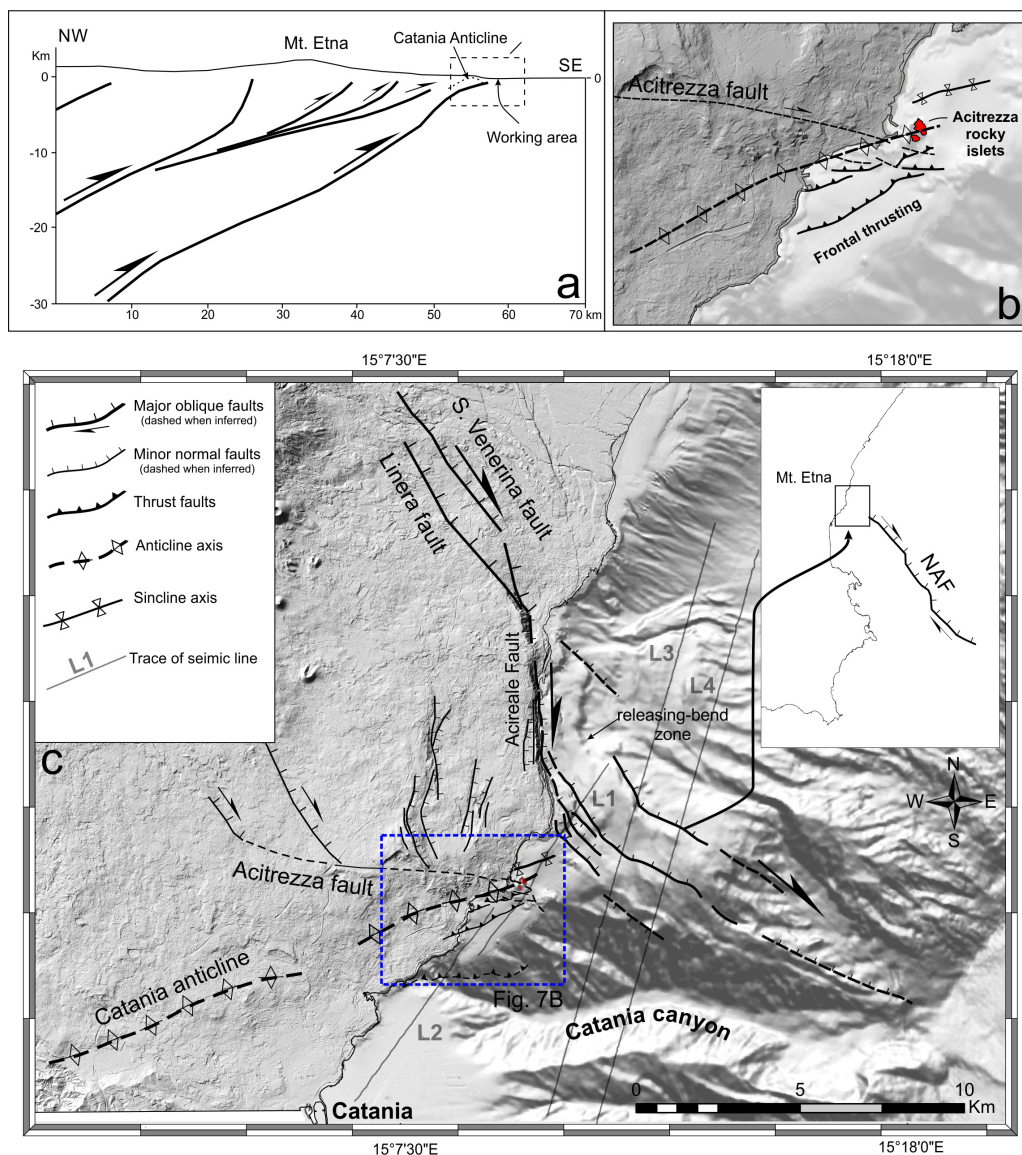


Figure 7. Tectonic interpretation of the investigated area based on high-resolution seismic profiles and available multibeam data [11]. (a) Reconstructed crustal section across Mt. Etna and the Catania Anticline (see Figure 1 a for location), showing the location of the contractional structures at the front of a deep-seated thrust ramp (see also [17,23]); (b) In the Acitrezza offshore, ENE-WSW trending reverse faults deform the continental shelf. These structures are coaxial to the hinge of the Catania Anticline and, therefore, they have been interpreted as its frontal thrusting; (c) Towards the NE, the detected extensional fault system appears nucleated within a releasing zone formed at bending of a major transtensional faults. The latter include the seismogenic Timpe Fault System, here interpreted as the continuation toward the mainland of the North Alfeo Fault [13].

5. Discussion

Our analysis together with published seismological and geodetic data [17], suggest that a compressive regime currently occurs at crustal depth below Mt. Etna, accommodated by shallow thrusting and folding at the front of the chain, south of the volcanic edifice (Figure 7a). According to [17], the accumulated compressive stress is released through earthquakes along the thrust ramps in the

inner sector of the chain, whereas it is accommodated by aseismic deformation at the front, where incipient detachment thrusting occurs within the clayish foredeep deposits [62]. Reverse faults and folding detected in the high-resolution seismic profiles can be framed in this tectonic setting and interpreted as the offshore prolongation of the large WSW-ENE trending anticline growing north of Catania (the Catania Anticline, Figure 7c).

Radiometric dating of measured paleo shorelines occurring along the coastline between Catania and Aci Trezza [15] suggests an uplift rate of ~3 mm/yr in the last 4 ka in correspondence of the fold hinge. Moreover, a NNW-SSE oriented axis of compression has been inferred by earthquake focal mechanisms. These data are consistent with GPS measurements over the last 20 years at the front of the chain, which have also revealed a shortening rate of ~5 mm/yr [17,63]. The Catania Anticline has also been interpreted as the result of gravitational spreading of the volcanic edifice [9,10]. Our interpretation as a tectonic contractional structure is more plausible considering that this anticline is sub-parallel to the Terreforti anticline (Figure 1b).

Seismic profiles highlight extensional structures that bound to the east the contractional system, along the offshore extension of the transtensional Timpe Fault System. The extensional structures dislocate the 220–120 ka volcanic plateau, giving rise to Middle-Upper Pleistocene-Holocene wedge-shaped syn-tectonic basins and seafloor ruptures. In particular, the NW-SE trending extensional structures connect on-land with the ~N-S trending Acireale Fault that, in turn, switches to NW-SE direction, giving rise to a seismogenic oblique-dextral fault system (the Linera-Santa Venerina fault system [19,21]). The geometry of the whole system, constituted by NW-SE major transtensional faults and ~N-S trending normal segments, can be interpreted as a releasing bend (Figure 7c) formed along the coastal sector of the Alfeo-Etna Fault System. This fault pattern is also in agreement with data derived from multibeam bathymetry [11,64] and multichannel seismic profiles [51] and it is very similar to that recently detected in the bathyal plain by [13] (see inset in Figure 7c). Taking into account their location, trend and kinematics, these faults could represent the landward prosecution of a major kinematic boundary inferred from high-penetration seismic profiles acquired in the Ionian Sea (inset in Figure 7c; the north Alfeo Fault System of [13]; the Alfeo-Etna Fault System [14]), rather than the on-land expression of the Malta Escarpment as stated by previous studies (e.g., [65]). The current tectonic activity of this belt is also suggested by crustal seismicity on-land [18,20,41] and offshore [14].

High rates of lithospheric extension in this sector of the Ionian Sea (see [29]) have also favoured ascents of fluids (Figures 3e and 4b) and magmas, similar to those outcropping in the Aci Trezza rocky islets. They probably intruded along highly fractured and damaged fault zones forming continuous NW-SE trending ridges sub-parallel to the tectonic structures, as suggested by multibeam data [11].

It is worth to note that the investigated coastal sector is characterised by long- (since LGM) and short-term tectonic uplift that is in contrast with the general seaward sliding dynamics (see also [15] and [44]). In particular, the GPS and interferometry data [7,9,10] reveal an apparent vertical stability of the coastal sector at the footwall of the Acireale Fault (Figure 1b), providing evidence that the subsidence related to the sliding process compensates for the regional and fault-related uplift. Conversely, to the south (between Capo Mulini and Catania, Figure 1b) a general uplift of the coast during the last post-LGM is observed [15], highlighting an acceleration of the vertical motion at the hinge of the Catania Anticline, in contrast with the seaward sliding (Figure 7b). Moreover, in spite of the Aci Trezza Fault being considered the southern boundary of the Mt. Etna eastern sliding sector [12], no evidences of sliding-related structures (e.g., disturbed sediments) are documented in literature. Conversely, growth fault patterns in nearby sediments indicate the tectonic origin of the identified structures. This can be explained by assuming that the sliding process has only recently superimposed to the long-term volcano-tectonic and regional uplifting [15].

6. Conclusions

High-resolution seismic profiles coupled with constraints derived from structural modelling and bathymetric map have provided new insights into the active tectonics of a sector of Mt. Etna offshore. The main outcomes of this study can be summarized as follows:

- the occurrence of contractional and extensional structures active since the Middle Pleistocene suggests that the deformation of the SE offshore margin of Mt. Etna must be related not only to gravity sliding, as previously stated but also to regional-scale tectonic processes;
- the Aci Trezza offshore area has experienced continuous shortening from the Middle Pleistocene to Present. The long-term rate of convergence was estimated in ~ 0.5 mm/yr in the last 220 ka, which is consistent with geodetic regional shortening measured along the front of the Sicilian chain. WNW-ESE trending contractional structures are interpreted as frontal splays of active detachment folds, aseismically growing in the northern outskirts of Catania;
- active extensional faults occur NE of the contractional structures; these correspond to the seaward prolongation of the NW-SE trending transtensional Timpe Fault System and has favoured fluids intrusions;
- seismic profiles and bathymetric map coherently indicate that the NW-SE trending extensional fault system turn to N-S direction near the Ionian coastline and it connects with the Timpe Fault System on-land, forming, as a whole, a releasing-bend zone;
- our data highlight that active contractional and extensional tectonic processes coexist in the south-eastern sector of Mt. Etna and prevail over flank sliding processes; thrust and folding can be related to the late migration of the Sicilian thrust-belt front, whereas oblique faulting to the east is probably part of the major kinematic boundary located in the western Ionian Sea.

Acknowledgments: Two anonymous reviewers are kindly acknowledged for their constructive comments and suggestions. This work was funded by a DPC-INGV 2012 grant, Project V3 “Multi-disciplinary analysis of the relationship between tectonic and volcanic activity” and by PRIN 2010-11 Project “Active and recent geodynamics of Calabrian Arc and accretionary complex in the Ionian Sea” (responsible C. Monaco) and by grant of University of Catania, project “Multidisciplinary analysis of the deformation in the around of active tectonic structures (responsible G. Barreca). High-resolution single channel (sparker) reflection seismic data were acquired onboard the R/V Neptune 1 GeoNautics. The authors would also like to thank Alfonso Analfino for his assistance during the seismic data acquisition. We thank Midland Valley Ltd. for providing the academic license of Move and software support. Seismic data were processed by using the RadexPro and the GeoSuite AllWork software packages.

Author Contributions: Giovanni Barreca and Carmelo Monaco conceived the study by planning the offshore seismic survey. Giovanni Barreca, Carmelo Monaco and Fabrizio Pepe organized the seismic survey and acquired the seismic data. Fabrizio Pepe and Marta Corradino carry out seismic data processing and seismo-stratigraphic interpretation. Giovanni Barreca, Carmelo Monaco and Fabrizio Pepe performed structural interpretation of seismic data and wrote the draft of the manuscript. All the authors contributed to the final version of the manuscript.

Conflicts of Interest: The authors declare no conflict of interest.

References

1. Palano, M.; Ferranti, L.; Monaco, C.; Mattia, M.; Aloisi, M.; Bruno, V.; Cannavò, F.; Siligato, G. GPS velocity and strain fields in Sicily and southern Calabria, Italy: Updated geodetic constraints on tectonic block interaction in the central Mediterranean. *J. Geophys. Res.* **2012**, *117*, B07401. [[CrossRef](#)]
2. Branca, S.; Coltelli, M.; De Beni, E.; Wijbrans, J. Geological evolution of Mount Etna volcano (Italy) from earliest products until the first central volcanism (between 500 and 100 ka ago) inferred from geochronological and stratigraphic data. *Int. J. Earth Sci.* **2007**, *97*, 135–152. [[CrossRef](#)]
3. Azzaro, R.; Bonforte, A.; Branca, S.; Guglielmino, F. Geometry and kinematics of the fault systems controlling the unstable flank of Etna volcano (Sicily). *J. Volcan. Geother. Res.* **2013**, *251*, 5–15. [[CrossRef](#)]

4. Rasà, R.; Azzaro, R.; Leonardi, O. Aseismic creep on faults and flank instability at Mt. Etna Volcano, Sicily. In *Volcano Instability on the Earth and Other Planets*; McGuire, W.C., Jones, A.P., Neuberg, J., Eds.; Special Publications; Geological Society: London, UK, 1996; Volume 110, pp. 179–192.
5. Rust, D.; Neri, M. The boundaries of large-scale collapse on the flanks of Mount Etna, Sicily. In *Volcano Instability on the Earth and Other Planets*; McGuire, W.C., Jones, A.P., Neuberg, J., Eds.; Special Publications; Geological Society: London, UK, 1996; Volume 110, pp. 193–208.
6. Puglisi, G.; Bonforte, A. Dynamics of Mount Etna volcano inferred from static and kinematic GPS measurements. *J. Geophys. Res.* **2004**, *109*, B11404. [[CrossRef](#)]
7. Bonforte, A.; Puglisi, G. Dynamics of the eastern flank of Mount Etna volcano (Italy) investigated by a dense GPS network. *J. Volcanol. Geotherm. Res.* **2006**, *153*, 357–369. [[CrossRef](#)]
8. Froger, J.L.; Merle, O.; Briole, P. Active spreading and regional extension at Mount Etna imaged by SAR interferometry. *Earth Planet. Sci. Lett.* **2001**, *148*, 245–258. [[CrossRef](#)]
9. Lundgren, P.; Casu, F.; Manzo, M.; Pepe, A.; Berardino, P.; Sansosti, E.; Lanari, R. Gravity and magma induced spreading of Mount Etna volcano revealed by satellite radar interferometry. *Geophys. Res. Lett.* **2004**, *31*. [[CrossRef](#)]
10. Bonforte, A.; Guglielmino, F.; Coltelli, M.; Ferretti, A.; Puglisi, G. Structural assessment of Mount Etna volcano from Permanent Scatterers analysis. *Geochem. Geophys. Geosyst.* **2011**, *12*. [[CrossRef](#)]
11. Chiocci, L.F.; Coltelli, M.; Bosman, A.; Cavallaro, D. Continental margin large-scale instability controlling the flank sliding of Etna volcano. *Earth Planet. Sci. Lett.* **2011**, *305*, 57–64. [[CrossRef](#)]
12. Gross, F.; Krastel, S.; Geersen, J.; Hinrich, B.J.; Ridente, D.; Chiocci, F.L.; Bialas, J.; Papenberg, C.; Cukur, D.; Urlaub, M.; et al. The limits of seaward spreading and slope instability at the continental margin offshore Mt Etna, imaged by high-resolution 2D seismic data. *Tectonophysics* **2016**, *667*, 63–76. [[CrossRef](#)]
13. Gutscher, M.; Dominguez, S.; Mercier de Lepinay, B.; Pinheiro, L.; Gallais, F.; Babonneau, N.; Cattaneo, A.; Le Faou, Y.; Barreca, G.; Micallef, A.; et al. Tectonic expression of an active slab tear from high-resolution seismic and bathymetric data offshore Sicily (Ionian Sea). *Tectonics* **2015**, *34*. [[CrossRef](#)]
14. Polonia, A.; Torelli, L.; Artoni, A.; Carlini, M.; Faccenna, C.; Ferranti, L.; Gasperini, L.; Govers, R.; Klaeschen, D.; Monaco, C.; et al. The Ionian and Alfeo-Etna fault zones: New segments of an evolving plate boundary in the central Mediterranean Sea? *Tectonophysics* **2016**, *675*, 69–90. [[CrossRef](#)]
15. Branca, S.; De Guidi, G.; Lanzafame, G.; Monaco, C. Holocene vertical deformation along the coastal sector of Mt. Etna volcano (eastern Sicily, Italy): Implications on the timespace constrains of the volcano lateral sliding. *J. Geodyn.* **2014**, *82*, 194–203. [[CrossRef](#)]
16. Labaume, P.; Bousquet, J.C.; Lanzafame, G. Early deformations at a submarine compressive front: The Quaternary Catania foredeep south of Mt. Etna, Sicily, Italy. *Tectonophysics* **1990**, *177*, 349–366. [[CrossRef](#)]
17. De Guidi, G.; Barberi, G.; Barreca, G.; Bruno, V.; Cultrera, F.; Grassi, S.; Imposa, S.; Mattia, M.; Monaco, C.; Scarfi, L.; et al. Geological, seismological and geodetic evidence of active thrusting and folding south of Mt. Etna (eastern Sicily): Revaluation of “seismic efficiency” of the Sicilian Basal Thrust. *J. Geodyn.* **2015**, *90*, 32–41. [[CrossRef](#)]
18. Monaco, C.; Tapponnier, P.; Tortorici, L.; Gillot, P.Y. Late Quaternary slip rates on the Acireale-Piedimonte normal faults and tectonic origin of Mt. Etna (Sicily). *Earth Planet. Sci. Lett.* **1997**, *147*, 125–139. [[CrossRef](#)]
19. Monaco, C.; De Guidi, G.; Ferlito, C. The Morphotectonic map of Mt. Etna. *Ital. J. Geosci.* **2010**, *129*, 408–428.
20. Azzaro, R. Earthquake surface faulting at Mount Etna volcano (Sicily) and implications for active tectonics. *J. Geodyn.* **1999**, *28*, 193–213. [[CrossRef](#)]
21. Mattia, M.; Bruno, V.; Caltabiano, T.; Cannata, A.; Cannavò, F.; D’Alessandro, W.; Di Grazia, G.; Federico, C.; Giammanco, S.; La Spina, A.; et al. A comprehensive interpretative model of slow slip events on Mt. Etna’s eastern flank. *Geochem. Geophys. Geosyst.* **2015**, *16*, 635–658. [[CrossRef](#)]
22. Monaco, C. Tettonica pleistocenica nell’area a sud dell’Etna (Sicilia orientale). *Ital. J. Quat. Sci.* **1997**, *10*, 393–398.
23. Lavecchia, G.; Ferrarini, F.; De Nardis, R.; Visini, F.; Barbano, M.S. Active thrusting as a possible seismogenic source in Sicily (Southern Italy): Some insights from integrated structural-kinematic and seismological data. *Tectonophysics* **2007**, *445*, 145–167. [[CrossRef](#)]

24. Bousquet, J.C.; Lanzafame, G. The tectonics and geodynamic of Mt. Etna: Synthesis and interpretation of geological and geophysical data. In *Mt. Etna: Volcano Laboratory*; Bonaccorso, A., Calvari, S., Coltelli, M., Del Negro, C., Falsaperla, S., Eds.; American Geophysical Union: Washington, DC, USA, 2004; Volume 143, pp. 29–47.
25. Lanzafame, G.; Bousquet, J.C. The Maltese escarpment and its extension from Mt. Etna to the Aeolian Islands (Sicily): Importance and evolution of a lithosphere discontinuity. *Acta Vulcanol.* **1997**, *9*, 113–120.
26. Bianca, M.; Monaco, C.; Tortorici, L.; Cernobori, L. Quaternary normal faulting in southeastern Sicily (Italy): A seismic source for the 1693 large earthquake. *Geophys. J. Int.* **1999**, *139*, 370–394. [[CrossRef](#)]
27. Argnani, A.; Bonazzi, C. Malta Escarpment fault zone offshore eastern Sicily: Pliocene-Quaternary tectonic evolution based on new multichannel seismic data. *Tectonics* **2005**, *24*. [[CrossRef](#)]
28. Barreca, G.; Bruno, V.; Cultrera, F.; Mattia, M.; Monaco, C.; Scarfi, L. New insights in the geodynamics of the Lipari-Vulcano area (Aeolian Archipelago, southern Italy) from geological, geodetic and seismological data. *J. Geodyn.* **2014**, *182*, 150–167. [[CrossRef](#)]
29. Hirn, A.; Nicolich, R.; Gallart, J.; Laigle, M.; Cernobori, L. Roots of Etna volcano in faults of great earthquakes. *Earth Planet. Sci. Lett.* **1997**, *148*, 171–191. [[CrossRef](#)]
30. Gvirtzman, Z.; Nur, A. The formation of Mount Etna as the consequence of slab rollback. *Nature* **1999**, *401*, 782–785. [[CrossRef](#)]
31. Doglioni, C.; Innocenti, F.; Mariotti, G. Why Mt Etna? *Terra Nova* **2001**, *13*, 25–31. [[CrossRef](#)]
32. Polonia, A.; Torelli, L.; Gasperini, L.; Mussoni, P. Active faults and historical earthquakes in the Messina Straits area (Ionian Sea). *Nat. Hazards Earth Syst. Sci.* **2012**, *12*, 2311–2328. [[CrossRef](#)]
33. Polonia, A.; Torelli, L.; Mussoni, P.; Gasperini, L.; Artoni, A.; Klaeschen, D. The Calabrian Arc subduction complex in the Ionian Sea: Regional architecture, active deformation, and seismic hazard. *Tectonics* **2011**, *30*. [[CrossRef](#)]
34. Gallais, F.; Gutscher, M.A.; Klaeschen, D.; Graindorge, D. Two-stage growth of the Calabrian accretionary wedge in the Ionian Sea (Central Mediterranean): Constraints from depth-migrated multichannel seismic data. *Mar. Geol.* **2012**, *326–328*, 28–45. [[CrossRef](#)]
35. Di Stefano, A.; Branca, S. Long-term uplift rate of the Etna volcano basement (southern Italy) based on biochronological data from Pleistocene sediments. *Terra Nova* **2001**, *14*, 61–68. [[CrossRef](#)]
36. Kieffer, G. Dépôts et niveaux marins et fluviaux de la région de Catane (Sicile). *Méditerranée* **1971**, *5–6*, 591–626. [[CrossRef](#)]
37. Ristuccia, G.M.; Di Stefano, A.; Gueli, A.M.; Monaco, C.; Stella, G.; Troja, S.O. OSL chronology of Quaternary terraced deposits outcropping between Mt. Etna volcano and the Catania Plain (Sicily, southern Italy). *Phys. Chem. Earth* **2013**, *63*, 36–46. [[CrossRef](#)]
38. De Beni, E.; Branca, S.; Coltelli, M.; Groppelli, G.; Wijbrans, J. ³⁹Ar/⁴⁰Ar isotopic dating of Etna volcanic succession. *Ital. J. Geosci.* **2011**, *130*, 292–305. [[CrossRef](#)]
39. Corsaro, R.A.; Neri, M.; Pompilio, M. Paleo-environmental and volcano-tectonic evolution of the southeastern flank of Mt. Etna during the last 225 ka inferred from the volcanic succession of the “Timpe”, Acireale, Sicily. *J. Volcanol. Geotherm. Res.* **2001**, *113*, 289–306. [[CrossRef](#)]
40. Azzaro, R.; Branca, S.; Gwinner, K.; Coltelli, M. The volcano-tectonic map of Etna volcano, 1:100.000 scale: An integrated approach based on a morphotectonic analysis from high-resolution DEM constrained by geologic, active faulting and seismotectonic data. *Ital. J. Geosci.* **2012**, *131*, 153–170. [[CrossRef](#)]
41. Azzaro, R.; Barbano, M.S.; Antichi, B.; Rigano, R. Macroseismic catalogue of Mt. Etna earthquakes from 1832 to 1998. *Acta Vulcanol.* **2000**, *12*, 3–36.
42. Monaco, C.; Catalano, S.; Cocina, O.; De Guidi, G.; Ferlito, C.; Gresta, S.; Musumeci, C.; Tortorici, L. Tectonic control on the eruptive dynamics at Mt. Etna volcano (eastern Sicily during the 2001 and 2002–2003 eruptions). *J. Volcanol. Geotherm. Res.* **2005**, *144*, 221–233. [[CrossRef](#)]
43. Alparone, S.; D’Amico, S.; Gambino, S.; Maiolino, V. Buried active faults in the Zafferana Etnea territory (south-eastern flank of Mt. Etna): Geometry and kinematics by earthquake relocation and focal mechanisms. *Ann. Geophys.* **2013**, *56*. [[CrossRef](#)]
44. Firth, C.; Stewart, I.; McGuire, W.M.; Kershaw, S.; Vita-Finzi, C. Coastal elevation changes in eastern Sicily: Implications for volcano instability at Mount Etna. In *Volcano Instability on the Earth and Other Planets*; McGuire, W.C., Jones, A.P., Neuberg, J., Eds.; Special Publications; Geological Society: London, UK, 1996; Volume 110, pp. 153–167.

45. Stewart, I.; Cundy, A.; Kershaw, S.; Firth, C. Holocene coastal uplift in the Taormina area, northeastern Sicily: Implications for the southern prolongation of the Calabrian seismogenic belt. *J. Geodyn.* **1997**, *24*, 37–50. [[CrossRef](#)]
46. Antonioli, F.; Kershaw, S.; Rust, R.; Verrubbi, V. Holocene sea-level change in Sicily and its implications for tectonic models: New data from the Taormina area, northeast Sicily. *Mar. Geol.* **2003**, *196*, 53–71. [[CrossRef](#)]
47. Antonioli, F.; Ferranti, L.; Lambeck, K.; Kershaw, S.; Verrubbi, V.; Dai Pra, G. Late Pleistocene to Holocene record of changing uplift rates in southern Calabria and northeastern Sicily (southern Italy, Central Mediterranean Sea). *Tectonophysics* **2006**, *422*, 23–40. [[CrossRef](#)]
48. Branca, S. Geological and geomorphologic evolution of the Etna volcano NE flank and relationships between lava flow invasions and erosional processes in the Alcantara Valley (Italy). *Geomorphology* **2003**, *53*, 247–261. [[CrossRef](#)]
49. Spampinato, C.R.; Scicchitano, G.; Ferranti, L.; Monaco, C. Raised Holocene paleo-shorelines along the Capo Schisò coast, Taormina: New evidence of recent co-seismic deformation in northeastern Sicily (Italy). *J. Geodyn.* **2012**, *55*, 18–31. [[CrossRef](#)]
50. Acocella, V.; Puglisi, G.; Amelung, F. Flank instability at Mt. Etna Preface. *J. Volcanol. Geotherm. Res.* **2013**, *251*, 1–4. [[CrossRef](#)]
51. Argnani, A.; Mazzarini, F.; Bonazzi, C.; Bisson, M.; Isola, I. The deformation offshore of Mount Etna as imaged by multichannel seismic reflection profiles. *J. Volcanol. Geotherm. Res.* **2013**, *251*, 50–64. [[CrossRef](#)]
52. Tibaldi, A.; Groppelli, G. Volcano-tectonic activity along structures of the unstable NE flank of Mt. Etna (Italy) and their possible origin. *J. Volcanol. Geotherm. Res.* **2002**, *115*, 277–302. [[CrossRef](#)]
53. Ferranti, L.; Burrato, P.; Pepe, F.; Santoro, E.; Mazzella, M.E.; Morelli, D.; Passaro, S.; Vannucci, G. An active oblique-contractual belt at the transition between the Southern Apennines and Calabrian Arc: The Amendolara ridge, Ionian Sea, Italy. *Tectonics* **2014**, *33*, 2169–2194. [[CrossRef](#)]
54. Loreto, M.F.; Pepe, F.; De Ritis, R.; Ventura, G.; Ferrante, V.; Speranza, F.; Tomini, I.; Sacchi, M. Geophysical investigation of Pleistocene volcanism and tectonics offshore Capo Vaticano (Calabria, southeastern Tyrrhenian sea). *J. Geodyn.* **2015**, *90*, 71–86. [[CrossRef](#)]
55. Damuth, J.E. Use of high-frequency (3.5–12 kHz) echograms in the study of near-bottom sedimentation processes in the deep-sea: A review. *Mar. Geol.* **1980**, *38*, 51–75. [[CrossRef](#)]
56. Lambeck, K.; Antonioli, F.; Anzidei, M.; Ferranti, L.; Leoni, G.; Scicchitano, G.; Silenzi, S. Sea level change along the Italian Coast during the Holocene projections for the future. *Quat. Int.* **2011**, *232*, 250–257. [[CrossRef](#)]
57. Spratt, R.M.; Lisiecki, L.E. A Late Pleistocene sea level stack. *Clim. Past* **2016**, *12*, 1079–1092. [[CrossRef](#)]
58. Clark, P.U.; Dyke, A.S.; Shakun, J.D.; Carlson, A.E.; Clark, J.; Wohlfarth, B.; Mitrovica, J.X.; Hostetler, S.W.; McCabe, A.M. The Last Glacial Maximum. *Science* **2009**, *325*, 710–714. [[CrossRef](#)] [[PubMed](#)]
59. Oba, T.; Irino, T. Sea level at the last glacial maximum, constrained by oxygen isotopic curves of planktonic foraminifera in the Japan Sea. *J. Quat. Sci.* **2012**, *27*, 941–947. [[CrossRef](#)]
60. Cacho, I.; Grimallt, J.O.; Pelejerlo, C.; Canals, M.; Sierro, F.J.; Flores, J.A.; Shackleton, N. Dansgaard-Oeschger and Heinrich event imprints in Alboran Sea paleotemperatures. *Paleoceanography* **1999**, *14*, 698–705. [[CrossRef](#)]
61. Somoza, L.; Medialdea, T.; León, R.; Ercilla, G.; Vázquez, J.T.; Farran, M.; Hernández-Molina, J.; González, J.; Juan, C.; Fernández-Puga, M.C. Structure of mud volcano systems and pockmarks in the region of the Ceuta Contourite Depositional System (Western Alborán Sea). *Mar. Geol.* **2012**, *332–334*, 4–26. [[CrossRef](#)]
62. Torelli, L.; Grasso, M.; Mazzoldi, G.; Peis, D. Plio-Quaternary tectonic evolution and structure of the Catania foredeep, the northern Hyblean Plateau and the Ionian shelf (SE Sicily). *Tectonophysics* **1998**, *298*, 209–221. [[CrossRef](#)]
63. Mattia, M.; Bruno, V.; Cannavò, F.; Palano, M. Evidences of a contractional pattern along the northern rim of the Hyblean Plateau (Sicily, Italy) from GPS data. *Geol. Acta* **2012**, *10*, 1–9.

64. Cavallaro, D.; Bosman, A.; Chiocci, F.; Coltelli, M. A new morphobathymetric analysis of the submarine features in the neighbourhood of Acitrezza, Catania (Italy). In Proceedings of the Abstract Book of Meeting “Tethys to Mediterranean, a Journey of Geological Discovery”, Catania, Italy, 3–5 June 2008; p. 36.
65. Monaco, C.; Petronio, L.; Romanelli, M. Tettonica estensionale nel settore orientale del Monte Etna (Sicilia): DATI morfotettonici e sismici. In Proceedings of the Atti del Convegno Geodinamica e Tettonica Attiva del Sistema Tirreno-Appennino, Camerino, Italy, 9–10 February 1995; pp. 363–374.



© 2018 by the authors. Licensee MDPI, Basel, Switzerland. This article is an open access article distributed under the terms and conditions of the Creative Commons Attribution (CC BY) license (<http://creativecommons.org/licenses/by/4.0/>).